Report no. changed (Mar 2006): SM-415-UU

NATO OTAN

NATO UNDERSEA RESEARCH CENTRE REPORT

A study of the uncertainty in estimate seabed properties as a result of geoacoustic inversion algorithms

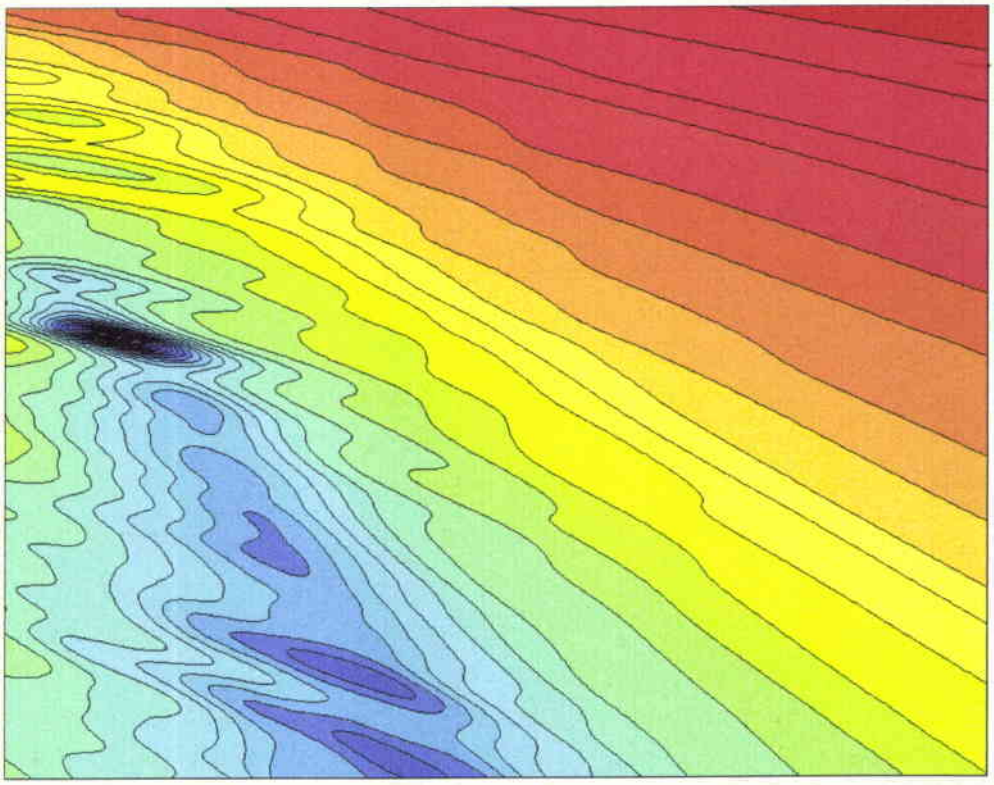

Mark Fallat
Stan Dosso
Peter L. Nielsen

October 2003

MEMORANDUM serial no: SM-415

NORTH ATLANTIC TREATY ORGANIZATION ORGANISATION DU TRAITE DE L'ATLANTIQUE NORD

A study of the uncertainty in estimated seabed properties as a result of geoacoustic inversion algorithms.

Mark Fallat, Stan Dosso and Peter L. Nielsen

The content of this document pertains to work performed under Project 04C-1 of the SACLANTCEN Programme of Work. The document has been approved for release by The Director, SACLANTCEN.

Steven E. Ramberg
Director

intentionally blank page

A study of the uncertainty in estimated seabed properties as a result of geoacoustic inversion algorithms.

Mark Fallat, Stan Dosso and Peter L. Nielsen

Executive Summary:

In the littoral environment, geoacoustic properties of the seafloor can have a significant influence on acoustic propagation. Much effort has been devoted to the estimation of seafloor properties. Geoacoustic inversion techniques can provide accurate estimates of the environmental properties for most littoral environments. The disadvantage is that these methods often require many assumptions to be made in order to make the problem tractable. These assumptions include the description of the environmental model, water column properties, experimental geometry, range-dependence, etc. Another thing that is taken for granted is that the algorithm used will provide the correct answer. Geoacoustic inversion is a very difficult, multi-dimensional, non-linear optimization problem and the algorithms used often have limitations.

In this report, an investigation of algorithm-induced uncertainty in geoacoustic inversion results is described. Three inversion algorithms (fast simulated annealing, genetic algorithms, adaptive simplex simulated annealing) are evaluated with an emphasis on performance and on the level of uncertainty induced by the algorithms. The algorithms are evaluated by performing multiple inversions of synthetic data (noise-free and noisy) and acoustic data measured during the MAPEX 2000 experiment.

intentionally blank page

A study of the uncertainty in estimated seabed properties as a result of geoacoustic inversion algorithms.

Mark Fallat, Stan Dosso and Peter L. Nielsen

Abstract:

This paper investigates the inherent uncertainty in estimated seabed properties derived from matched-field geoacoustic inversion algorithms. This algorithm-induced uncertainty must be considered when interpreting inversion results in terms of environmental changes as a function of time or space (eg., water column changes or range dependence). Fast simulated annealing (FSA), genetic algorithms (GA), and adaptive simplex simulated annealing (ASSA) are compared by performing multiple inversions of synthetic data (noise-free and noisy) and acoustic data measured over two areas with different sediment types. ASSA is shown to produce the lowest uncertainty in inversion results for all cases, followed by GA and FSA. For one the sediment types the uncertainty is essentially negligible, while for the other case the uncertainty is significant compared to environmental variations reported in the literature.

Keywords: Geoacoustic Inversion ○ Variability ○ Uncertainty ○ Matched Field Inversion ○ Fast Simulated Annealing ○ Genetic Algorithms ○ Adaptive Simplex Simulated Annealing

Contents

1

Introduction

In the past decade, considerable effort has been applied to the problem of estimating environmental parameters from measured ocean acoustic data. Geoacoustic inversion provides a convenient method for determining *in situ* seabed parameters with a sensitivity relevant to sonar applications. Many approaches have been applied in geoacoustic inversion but the most popular is matched field inversion (MFI) [1]. Conceptually, MFI represents a straightforward modeling approach to inversion, based on searching for environmental parameters that minimize the mismatch between measured and modeled acoustic fields. However, difficulties arises from the fact that geoacoustic inversion is strongly non-linear with large parameter spaces that often contain many local minima. To successfully utilize MFI for geoacoustic characterization, an efficient and effective parameter search algorithm is required.

A variety of search algorithms have been applied to the geoacoustic MFI. Global optimization methods such as simulated annealing (SA) and its variants [2–5] and genetic algorithms (GA) [6–9] are two of the more commonly used algorithms. Recently, hybrid methods [7, 10–12] which combine a global optimization with some form of local (gradient-based) search procedure have also been applied. Inter-parameter correlations which result in oblique valleys in the parameter space provide particularly challenging cases for MFI. Hybrid methods navigate correlated parameter spaces via the local search component. Alternatively, parameter rotations to minimize correlations have been applied in SA inversion [5]. Two major workshops,with accompanying special journal issues [13, 14], have been dedicated specifically to investigating and comparing MFI algorithms using noise-free synthetic data.

Recently, geoacoustic inversion methods have been applied to assess temporal and spatial variability in the environment. For example, Siderius *et al.* [15] and Snellen*et al.* [16] considered geoacoustic inversion of vertical array data along a fixed path over a period of hours, and interpreted the uncertainty in the inversion results in terms of sensitivity to temporal variations in the ocean sound-speed profile. Siderius *et al.* [17] and Fallat *et al.* [18] considered the uncertainty of inversion results for towed array data in terms of spatially-varying seabed structure along the tow track. All of the above studies applied GA as the search algorithm.

Before conclusions on temporal or spatial variations can be drawn from geoacoustic inversion results, however, it is important to consider the uncertainty inherent in

the inversion procedure itself, i.e., the repeatability or consistency of results simply with different random initializations of the algorithm. Snellen *et al.* [16] investigated this by carrying out multiple GA inversions of (noise-free) simulated data. However, the actual uncertainty in inversion results can vary considerably between simulated data (noise-free and noisy) and measured data, and can also be a function of the inversion algorithm applied.

This paper investigates the uncertainty of three geoacoustic inversion algorithms for noise-free and noisy synthetic data from the 1997 Geoacoustic Inversion Workshop [13] and for measured data from the MAPEX 2000 experiment. The algorithms considered are GA fast simulated annealing (FSA) [19–21], and a hybrid inversion algorithm, adaptive simplex simulated annealing (ASSA) [10,12]. The FSA and ASSA algorithms were implemented by the authors while the inversion package SAGA [22] was employed for GA. SAGA has been applied extensively to such problems and is generally accepted as a standard geoacoustic inversion tool.

The remainder of this paper is organized as follows. Section 2 provides a brief overview of the three inversion algorithms. Section 3 presents the inversion results for noise-free and noisy synthetic test cases, and Sec. 4 presents the results for measured data. Finally, Sec. 5 summarizes and discusses this work.

2 Overview of Algorithms

This section provides a brief overview of the theory and implementation of the three inversion algorithms considered in this study. For a more complete description the reader is referred to the references provided.

2.1 Fast simulated annealing

Simulated annealing is a global optimization technique that can be used to determine a set of model parameters, $\mathbf{m} = \{m_i, i = 1, \cdots, M\}$ with bounds $m_i^- \leq m_i \leq m_i^+$, that minimizes an objective function $E(\mathbf{m})$. The method is based on an analogy to the thermodynamic process of annealing by which a system of atoms reaches its ground-state energy configuration through a procedure of heating and cooling slowly [23].

SA consists of a series of iterations involving random perturbations to the parameters. Perturbations that decrease the objective function E are always accepted. Perturbations that increase E are accepted conditionally, with a probability given by the Boltzman or Gibbs distribution:

$$P(\Delta E) = \exp(-\Delta E/T), \tag{1}$$

where T is a control parameter called temperature which is decreased slightly after each iteration. By accepting some perturbations that increase E the algorithm has the ability to escape local minima in search of a better solution. When T is high (in the early stages of inversion) the algorithm essentially searches the parameter space in a random manner. As T decreases, accepting increases in E become less probable, and the algorithm spends more time searching regions with lower values of E. Eventually the algorithm converges to a solution that should approximate the global minimum.

In this paper, fast simulated annealing [19–21] is employed. FSA is based on using a temperature-dependent Cauchy distribution to generate the parameter perturbations and reducing the temperature in a geometric manner. The Cauchy distribution

has the desirable properties of a Gaussian-like peak and Lorentzian tails which provide concentrated local sampling of the parameter space while attempting occasional large perturbations. The perturbation to each parameter is implemented according to

$$m_i = m_i^{'} + \xi \, \Delta_i \tag{2}$$

where $m_i^{'}$ is the model parameter prior to the perturbation and Δ_i is a random variable uniformly distributed on the interval $[-\Delta m_i, \Delta m_i]$, where $\Delta m_i = m_i^{+} - m_i^{-}$. The variable ξ is a Cauchy-distributed random variable defined by

$$\xi = T_j / T_0 \, \tan(\eta \, \pi / 2) \, , \tag{3}$$

where η is a uniform random number on $[-1, 1]$, T_j is the temperature at the j^{th} iteration and T_0 is the starting temperature. If a perturbation results in a parameter value outside the bounds, it is discarded and a new perturbation is drawn.

2.2 Adaptive simplex simulated annealing

Adaptive simplex simulated annealing [10,12] is a hybrid optimization algorithm that combines the downhill simplex method (DHS) with FSA. The resulting algorithm has proved more efficient and effective than either of the individual algorithms. Before describing ASSA, the DHS algorithm is briefly outlined.

The DHS algorithm is based on a intuitive geometric scheme for moving downhill in the parameter space [24,25]. Although DHS is not the most efficient algorithm for local downhill moves, it has the advantages of not computing partial derivatives or solving systems of equations. The algorithm operates on a simplex of $M + 1$ models in an M dimensional parameter space. The initial simplex is chosen at random and subsequently undergoes a series of transformations to move downhill. First, each model is ranked according to its objective function E from highest to lowest. The algorithm initially attempts to improve the model with the highest E value by reflecting it through the face of the simplex containing the model with the lowest E. If this new model has the lowest E, an extension by a factor of two in the same direction is attempted. If the reflection results in a model that still has the highest E, the move is rejected and a contraction by a factor of two is attempted. If none of the steps decrease the objective function, then a contraction by a factor of two in all dimensions toward the model with the lowest E is performed. This process is repeated until the E values for all models converge to within a user defined tolerance.

ASSA combines the DHS method and FSA in an adaptive optimization scheme. Unlike standard FSA, ASSA operates on a simplex of models rather than a single model, and instead of employing purely random perturbations to the model, a DHS step followed by a random perturbation is used to compute the new model parameters. The new model is then evaluated for acceptance using the same criteria as standard SA (1). The sizes of the random perturbations are determined adaptively, based on a running average of recently accepted perturbations. The perturbation scaling for each parameter is determined individually, and applied using the Cauchy distribution.

2.3 Genetic algorithms

Genetic algorithms are based on an analogy with the biological process of evolution [6]. GA seek to improve the fit between measured and modeled data of a population of models [23]. GA are based on five steps: coding, selection, crossover, mutation, and replacement. Coding consists of describing the model using a binary coding system that results in a "chromosome". The coding controls the resolution or discretization of the various parameters as well as the search space limits. In selection, pairs of models are selected to form the parents for the next generation. Selection is a random process with the probability of a model being selected increasing with its associated fit to the data. Once the appropriate number of parents have been selected a new population is generated via crossover. Crossover facilitates the distribution of genetic information between the selected models and the new population. Mutation is a random alteration of a single bit in the coded model, providing a mechanism for increasing the randomness of the population. Finally, replacement is the process of defining the new models for the next generation. Each new model is compared to a random model from the old population and the model with the best fit is retained. This has the advantage of providing the technique with a form of memory of good models.

By running the process of selection, crossover, mutation and replacement over many generations, the population of models becomes increasingly fit. The final population should therefore contain many good models which approximate the global minimum.

3

Synthetic Testcases

In this section, the three algorithms are evaluated using a synthetic testcase developed for the 1997 Matched Field Workshop [13]. The testcase involved determining the geometric and geoacoustic parameters for the environment shown in Fig. 1 where the form of the geoacoustic model was known to consist of a sediment layer over a semi-infinite basement. The inversions involved nine unknown parameters including the water depth, D, source range and depth, r and z, sediment thickness, h, sound speeds at the top and bottom of the sediment layer, c_0 and c_1 (linear gradient assumed), sound speed in the basement, c_2, and densities in the sediment and basement, ρ_s and ρ_b, respectively.

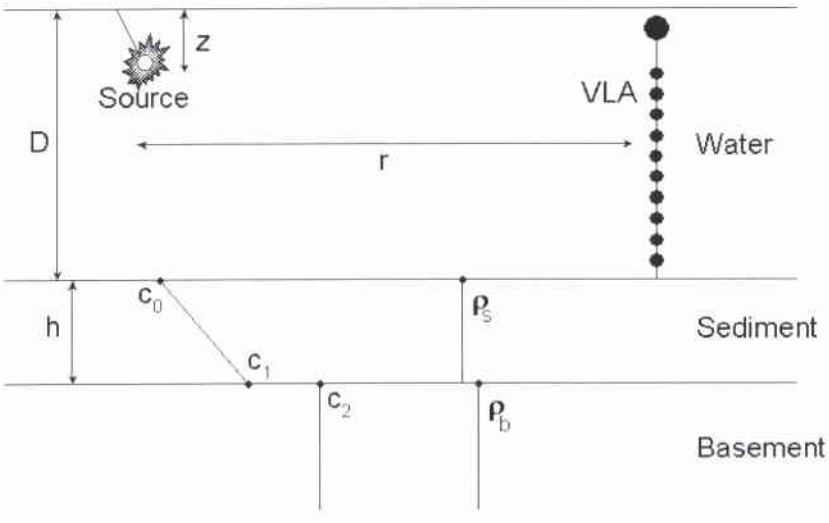

Figure 1 *Schematic diagram of the ocean environment used for the synthetic data inversions.*

The data used here consist of complex acoustic pressures at frequencies of 200–500 Hz in 50 Hz increments recorded at a vertical array of 40 hydrophones spanning

$\sim 2/3$ of the 115 m water column. Data and the replica fields were generated using the normal mode code ORCA [26]. The objective function used for the synthetic data inversions was based on the Bartlett processor [1] coherent in depth and summed incoherently in frequency (normalized to [0,1]). The algorithm evaluations involved both noise-free and noisy realizations of the synthetic data. For each data set several independent inversions were carried out to asses uncertainty in the results. The independent inversions were obtained by running inversions with different random starting models, different annealing schedules and, in some cases for GA, different discretizations for the parameter search intervals. Trial and error had shown that the number of forward model runs used in these studies provided a convergent solution for each of the algorithms.

3.1 Noise-free data

Figure 2 shows the inversion results for ASSA, GA and FSA for the noise-free synthetic data. For each algorithm, four independent inversions were carried out and the results displayed represent the model that obtained the lowest objective function value in each inversion.

The results from ASSA are consistently in excellent agreement with the true values for all parameters i.e., show essentially no uncertainty. The GA results show significantly more uncertainty about the true parameter values. One of the final models does approximate the true parameter values quite well with the exception of the basement density. Finally, the inversion results for FSA are the poorest of the three, although reasonable parameter values are obtained for at least one inversion. Table 1 summarizes the best inversion result for the three algorithms.

Table 1 *Summary of the best inversion results for the noise-free testcase.*

	D (m)	r (m)	z (m)	h (m)	c_0 (m/s)	c_1 (m/s)	c_2 (m/s)	ρ_s (g/cm^3)	ρ_b (g/cm^3)	Objective Function
True	115.33	2220	26.40	27.08	1516.0	1573.0	1751.0	1.54	1.85	
ASSA	115.33	2220	26.40	27.08	1516.0	1573.0	1751.0	1.54	1.85	1.8×10^{-10}
GA	115.28	2217	26.38	27.32	1516.1	1574.3	1764.7	1.54	1.70	2.8×10^{-4}
FSA	115.69	2209	26.32	25.62	1518.5	1563.9	1675.7	1.63	1.89	6.5×10^{-3}

The outliers in h and c_1 that occur in the GA and FSA results in Fig. 2 can be explained in terms of a (positive) correlation between these two parameters. Figure 3 shows a 2-D cross section of the log of the objective function versus h and c_1 (all other parameters held at true values). This figure illustrates the correlation, which is characterized by a narrow oblique valleys intersected by local minima. The correlation for this testcase has been discussed previously [10, 28], and has

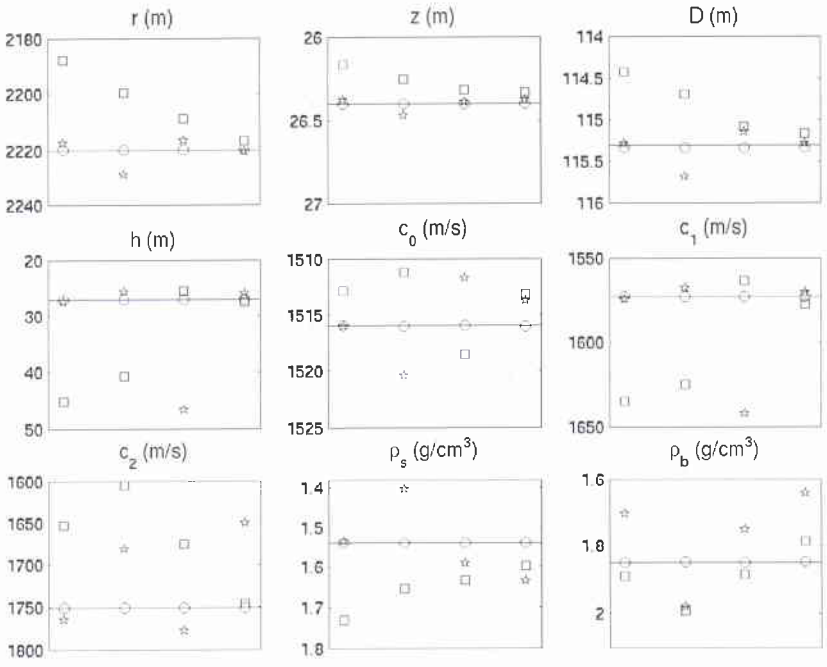

Figure 2 *Inversion results for the noise-free testcase. The inversion results for ASSA are represented by the circles, for GA by the stars and for FSA by the squares. The solid line in each panel represents the true parameter value.*

also been observed for experimental data [27, 29]. A weak positive correlation also exists between r and D. It should be noted that ASSA overcomes these correlations because it is sensitive to the multi-dimensional gradient information through the local component of the algorithm (DHS).

The relative sensitivity of the parameters in this benchmark problem have been discussed at length in a number of previous works [8, 10, 13, 21]. Essentially, the geometric parameters have the highest sensitivity, followed by sound speeds and layer thicknesses, with densities of lowest sensitivity.

3.2 Noisy data

Although the 1997 workshop utilized noise-free data, to provide a more realistic evaluation of the inversion algorithms, Gaussian noise was added to the noise-free data. For these inversions, five different noise realizations with a signal to noise ratio of 10 dB at each frequency were generated. This has been found to represent a realistic

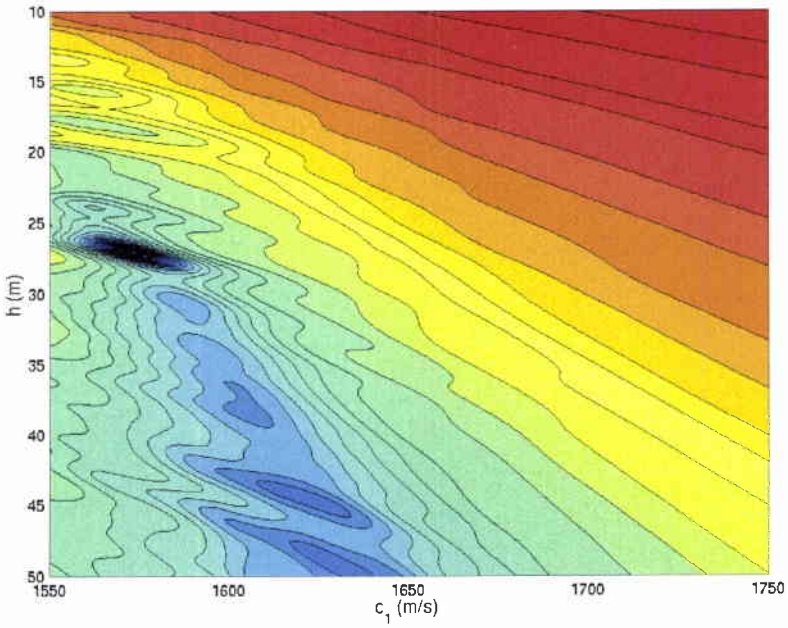

Figure 3 *2-D cross section of* $\log(E)$ *versus* h *and* c_1*, illustrating the strong correlation between these parameters. The blue areas represent low objective function values.*

level of noise (including experimental mismatch) [29]. To asses the uncertainty of the results, six independent inversions were carried out with each algorithm for each noise realization.

Figure 4 shows the final objective function values obtained for the inversions. The plots have been truncated to better demonstrate the differences in the objective function values; therefore, some of the FSA results with higher objective function values are not included. Also, some of the GA inversions obtained very similar objective function values using the same number of forward model evaluations and are plotted essentially on top of each other. ASSA obtained the lowest objective function values for most inversions (80%). Figure 4 shows that ASSA and GA both obtained lower objective functions values than FSA in all but one case. For the first, second and fifth noise realizations, several of the inversions become trapped in a local minimum with a higher objective function value than for the true parameters (solid line). This local minimum will be discussed in greater detail later. Note also that in several instances ASSA obtained objective function values lower than that for the true parameters. This is not a surprising results since noise has been added to the data and the true parameters, in some case, no longer represent the best estimate.

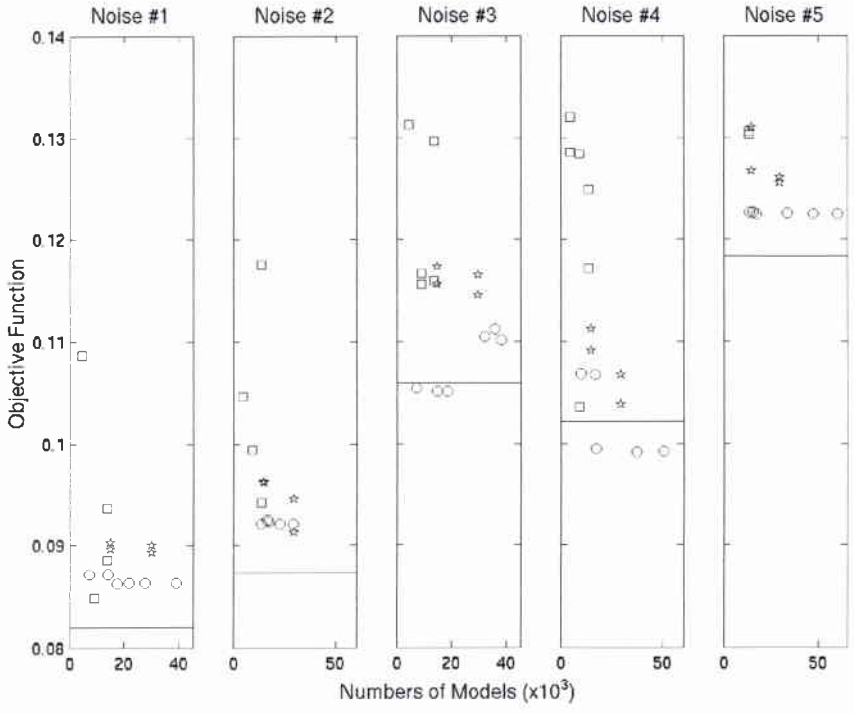

Figure 4 *Objective function values for the three algorithms and for the five different noise realizations (some FSA results with high objective function values are not shown). The inversion results for ASSA are represented by the circles, for GA by the stars and for FSA by the squares. The solid lines represent the objective function value for the true parameters.*

The inversion results for FSA, shown in Fig. 5, exhibit a large degree of uncertainty within each noise realization. Particular models appear to approximate the true parameter values for some of the most sensitive parameters, but in general the results are unstable.

Figure 6 shows the results obtained using ASSA. For most of the parameters the results are stable and closely approximate the true parameter value. While the results for ρ_b appear essentially random, due to the low sensitivity for this parameter, the results for h and c_1 indicate that ASSA is trapped in a local minimum due to the correlations between these parameters.

To further investigate this local minimum, the models that ASSA accepted during inversions of the third noise realization are plotted in Fig. 7. This plot includes the models for two independent inversions, one that closely approximated the true sediment parameters and one that converged to the local minimum. This figure represents a projection of all models in the multidimensional space onto the partic-

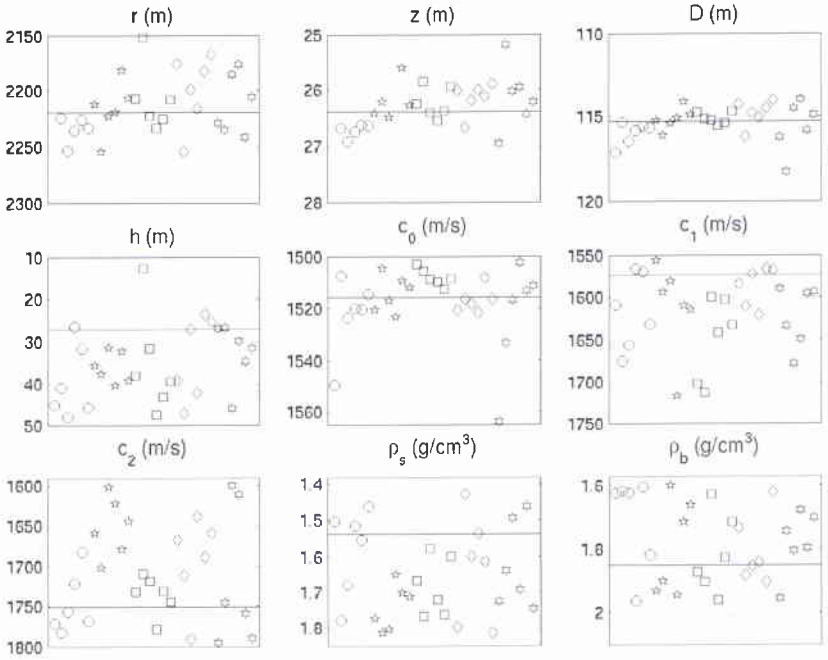

Figure 5 *FSA inversion results of the noisy synthetic data. Each symbol represents a different noise realization (six independent inversions per noise realization). Solid lines represent the true parameter values.*

ular parameter axis and can provide an impression of the overall multidimensional structure.

Figure 7 clearly demonstrates two well defined minima, one close to the true parameter values ($h \sim 27$ m, $c_1 \sim 1572$ m/s) and a broader one at higher values ($h \sim 47$ m, $c_1 \sim 1600$ m/s). These two minima result from the correlation between these parameters. Note that the objective function values at the two minima are almost identical, and differ by only 0.006 (for E normalized between [0,1]), indicating the strong non-uniqueness of this problem.

The inversion results for GA are presented in Fig. 8. For several of the parameters the agreement is quite good but in general the results are not as stable as for ASSA (Fig. 6). GA appears to become trapped in the local minima associated with h and c_1 described above, although not as frequently as ASSA. However, the uncertainty of results within a particular noise realization is generally larger for GA than ASSA.

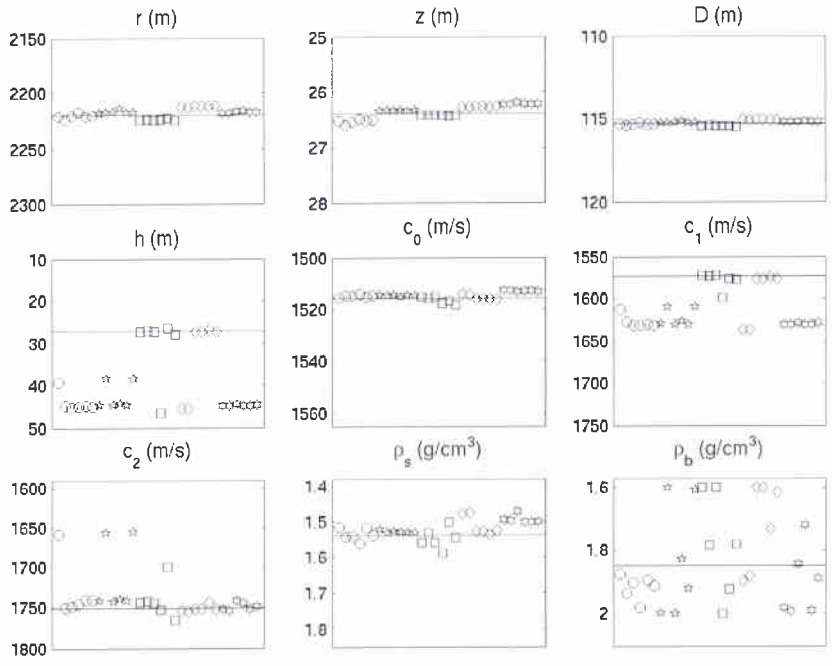

Figure 6 *ASSA inversion results for noisy synthetic data. Each symbol represents a different noise realization (six independent inversions per noise realization). Solid lines represent the true parameter values.*

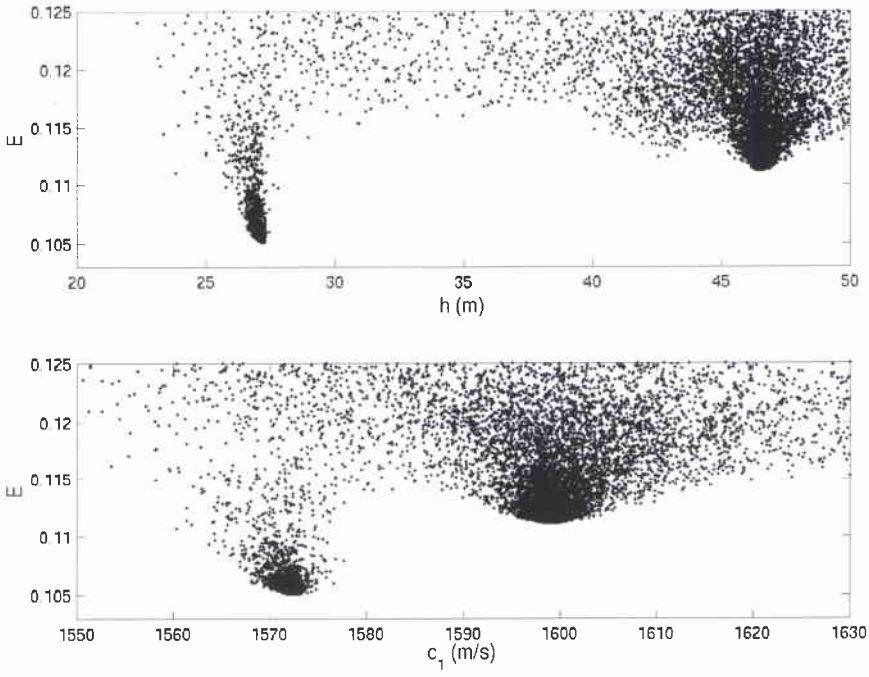

Figure 7 *Objective function E versus sediment layer thickness and sound speed at the bottom of the sediment for two independent ASSA inversions of the third noise realization. The plot has been truncated at low objective function values to better demonstrate the structure of the minima.*

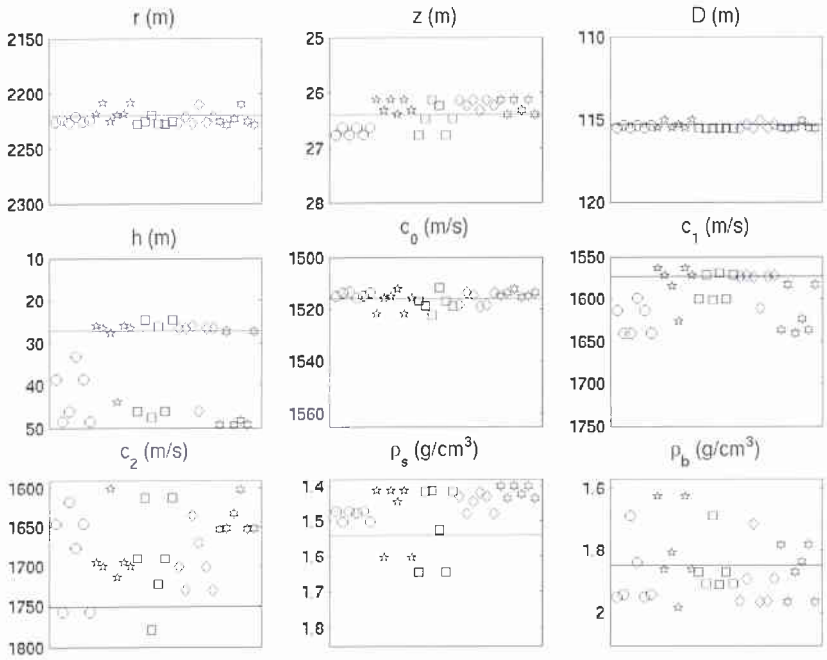

Figure 8 *GA inversion results for noisy synthetic data. Each symbol represents a different noise realization (six independent inversions per noise realization). Solid lines represent the true parameter values.*

4

Experimental Data Inversions

This section applies the inversion algorithms to data from the MAPEX 2000 experiment [17, 18]. Since it was evident from the synthetic inversions that FSA was not particularly effective, this method is not included in the comparison.

The data consists of 1-s linear frequency-modulated sweeps from 250–750 Hz (50-Hz increments) recorded on a towed horizontal line array (HLA) comprised of 64 elements spaced 4 m apart for a total acoustic aperture of 252 m. The range separation between the source and the head of the array was around 300 m. The source and array depths were both nominally 60 m. Figure 9 shows the experimental setup and the environmental model used for the inversions. Previous studies [17,18] have shown that for these data this model parameterization was suitable. The six unknown geoacoustic properties were the water depth, D, the sediment thickness, h, the sediment and basement sound speeds, c_s and c_b, and the density and attenuation of the entire seabed, ρ and α. Also included in the inversions were small corrections to the range and the source and receiver depths, but these parameters are not discussed here.

Two MAPEX 2000 data sets are considered in this paper. One was measured in an environment that was known to include a low-speed sediment layer, and the other was measured in an environment characterized by a more consolidated, higher-speed sediment (referred to as the low-speed and high-speed cases, respectively). Ten independent inversions were carried out for each data set. The objective function that was minimized was again based on the normalized Bartlett processor [1], except that is was summed coherently in frequency and incoherently over range.

Figure 10 shows the results of the ten independent inversions for the low-speed case. These results show considerable uncertainty for the water depth, sediment thickness and sediment sound speed. This is likely due to the difficulty in determining these parameters for a low-speed sediment layer which appears acoustically similar to the water column, leading to strong correlations between D, h and c_s [18,27]. In general, the results obtained using ASSA show less uncertainty for all parameters, and in particular for D, h, and c_s, than the results obtained using GA.

Figure 11 shows the inversion results for the high-speed case. These results show much less uncertainty for D, h, and c_s than for the low-speed case (Fig. 10). The

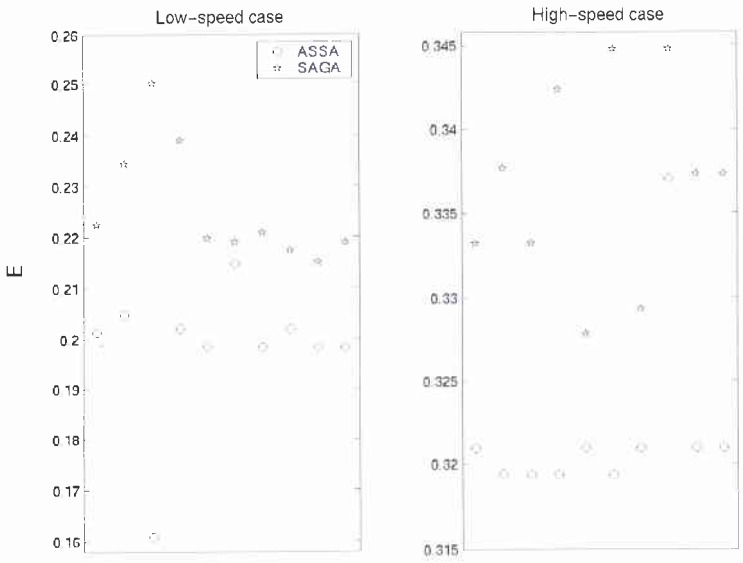

Figure 12 *Objective function values for the inversions of MAPEX 2000 data.*

Table 2 *Mean and average absolute variability (AV) of the inversion results for the MAPEX 2000 data.*

	Low-speed case				High-speed case			
Properties	ASSA		GA		ASSA		GA	
	Mean	AV	Mean	AV	Mean	AV	Mean	AV
D (m)	100.1	1.7	101.2	1.8	123.3	0.1	123.5	0.2
h (m)	6.9	1.7	5.6	1.9	19.8	0.1	19.4	0.3
c_s (m/s)	1466.2	14.6	1449.3	22.6	1566.3	0.2	1562.5	2.8
c_b (m/s)	1679.4	3.8	1680.9	12.8	1687.2	8.1	1685.0	8.5
ρ (g/cm^3)	1.29	0.06	1.31	0.08	1.15	0.0005	1.16	0.01
α (dB/λ)	0.04	0.008	0.14	0.1	0.07	0.005	0.08	0.02

5

Summary and Discussion

Geoacoustic inversion techniques are frequently utilized for estimating seabed properties from measured acoustic data. Algorithm-induced uncertainty represents an important issue in interpreting such inversion results in terms of spatial and/or temporal variation of the environment. The intent of this paper is to evaluate the uncertainty of results for three common geoacoustic inversion algorithms: fast simulated annealing (FSA), a hybrid inversion (adaptive simplex simulated annealing, ASSA), and genetic algorithms (GA). Synthetic benchmark testcases (noise-free and noisy) and experimental data (measured over low- and high-speed sediment layers) were considered.

In any comparison between algorithms it is important to ensure that an equal amount of care and attention is applied in running each algorithm. We have addressed this in part by considering a variety of control parameter settings for all three algorithms, we found that the conclusions of the study are not strongly dependent on these settings. Further, we point out that the authors have significant experience running all three inversion algorithms (e.g., see [3,10,12,18,21,27]). Finally, we consulted at length with the author of the GA package SAGA to ensure that it was run properly.

ASSA generally produced the lowest objective function values and the lowest uncertainty in the inversion results for all cases, followed by GA, with FSA producing results that were considerably poorer. The uncertainty differed considerably between noise-free synthetic data, noisy synthetic data, and the low- and high-speed measured-data cases. This indicates that the uncertainty should be evaluated on a case-by-case basis. For example, the algorithm-induced uncertainty for the high-speed case was likely negligible compared to other uncertainties. However, significant uncertainty was found for the low-speed case. In fact, the uncertainty for this case was comparable to that which has been interpreted as due to temporal and spatial uncertainty in previous studies [15–18]. The uncertainty in the results was exacerbated by inter-parameter correlations, which sometimes resulted in convergence to local minima.

Finally, it should be emphasized that the uncertainty inherent in inversion results (considered here) does not completely quantify the uncertainty of parameter estimates, which must also include consideration of the effects of data and theory errors mapped to uncertainty in model parameters [28,29].

References

[1] A. Tolstoy, *Matched Field Processing for Underwater Acoustics*, World Scientific, Pub. Co., New Jersey, 1993.

[2] M. D. Collins, W. A. Kuperman and H. Schmidt, "Nonlinear inversion for ocean-bottom properties," *J. Acoust. Soc. Am.* vol. 92, pp. 2770–2783, 1992.

[3] S. E. Dosso, M. L. Yeremy, J. M. Ozard and N. R. Chapman, "Estimation of ocean-bottom properties by matched-field inversion of acoustic field data," *IEEE J. Ocean. Eng.* vol. 18, pp. 232–239, 1993.

[4] C. E. Lindsay and N. R. Chapman, "Matched field inversion for geoacoustic model parameters using adaptive simulated annealing," *IEEE J. Ocean. Eng.* vol. 18, pp. 224–231, 1993.

[5] M. D. Collins and L. Fishman, "Efficient navigation of parameter landscapes," *J. Acoust. Soc. Am.* vol. 98, pp. 1637–1644, 1995.

[6] P. Gerstoft, "Inversion of seismo-acoustic data using genetic algorithms and *a posteriori* probability distributions," *J. Acoust. Soc. Am.* vol. 95, pp. 770–782, 1994.

[7] P. Gerstoft, "Inversion of acoustic data using a combination of genetic algorithms and the Gauss-Newton approach," *J. Acoust. Soc. Am.* vol. 97, pp. 2181–2190, 1995.

[8] G. J. Heard, D. Hannay and S. Carr, "Genetic algorithm inversion of the 1997 geoacoustic inversion workshop test case data," *J. Comp. Acoust.* vol. 6, pp. 61–71, 1998.

[9] M. Siderius, P. Gerstoft and P. Nielsen, "Broadband geoacoustic inversion from sparse data using genetic algorithms," *J. Comp. Acoust.* vol. 6, pp. 117–134, 1998.

[10] M. R. Fallat and S. E. Dosso, "Geoacoustic inversion via local, global and hybrid algorithms," *J. Acoust. Soc. Am.* vol. 105, pp. 3219–3230, 1999.

[11] M. Musil, M. J. Wilmut and N. R. Chapman, "A hybrid simplex genetic algorithm for estimating geoacoustic parameters using matched-field inversion," *IEEE J. Ocean. Eng.* vol. 24, pp. 358–369, 1999.

[12] S. E. Dosso, M. J. Wilmut and A-L. S. Lapinski, "An adaptive hybrid algorithm for geoacoustic inversion," *IEEE J. Ocean. Eng.* vol. 21, pp. 324–336, 2001.

[13] N. R. Chapman, A. Tolstoy and G. H. Brooke, "Workshop97: Benchmarking for geoacoustic inversion in shallow water," *J. Comp. Acoust.* vol. 6, pp. 1–28, 1998.

[14] N. R. Chapman, S. Chin-Bing, D. King and R. B. Evans, "Benchmarking geoacoustic inversion methods for range dependent waveguides," *IEEE J. Ocean. Eng.* To appear in July Issue vol. 28, 2003.

[15] M. Siderius, P. L. Nielsen, J. Sellschopp, M. Snellen and D. Simons, "Experimental study of geo-acoustic inversion uncertainty due to ocean sound-speed fluctuations," *J. Acoust. Soc. Am.* vol. 110, pp. 769–781, 2001.

[16] M. Snellen, D. Simons, M. Siderius, J. Sellschopp and P. L. Nielsen, "An evaluation of the accuracy of shallow water matched field inversion results," *J. Acoust. Soc. Am.* vol. 109, pp. 514–527, 2001.

[17] M. Siderius, P. L. Nielsen and P. Gerstoft, "Range-dependent seabed characterization by inversion of acoustic data from a towed receiver array," *J. Acoust. Soc. Am.* vol. 112, pp. 1523–1535, 2002.

[18] M. R. Fallat, P. L. Nielsen and M. Siderius, "Geoacoustic characterization of a range-dependent ocean environment using towed array data," *J. Acoust. Soc. Am.* (Submitted for publication), 2003.

[19] H. Szu and R. Hartley, "Fast simulated annealing," *Phys. Lett.* vol. A 122, pp. 157–162, 1987.

[20] P. Liu, S. Hartzell and W. Stephenson, "Non-linear multiparameter inversion using a hybrid global search algorithm: applications in reflection seismology," *Geophys. J. Int.* vol. 122, pp. 991–1000, 1995.

[21] M. R. Fallat and S. E. Dosso, "Geoacoustic inversion for the Workshop'97 benchmark test cases using simulated annealing," *J. Comp. Acoust.* vol. 6, pp. 29–43, 1998.

[22] P. Gerstoft, "SAGA Users manual 2.0, an inversion software package," Tech. Rep. SM–333, SACLANT Undersea Research Centre, La Spezia, Italy, 1997.

[23] M. Sen and P. L. Stoffa, *Global Optimization Methods in Geophysical Inversion*, Elsevier Science B. V., Amsterdam, The Netherlands, 1995.

[24] J. A. Nelder and R. Mead, "A simplex method for function minimization," *Computer Journal* vol. 7, pp. 308–311, 1965.

[25] W. H. Press, S. A. Teukolsky, W. T. Vetterling and B. P. Flannery, *Numerical Recipes*, Cambridge University Press, Cambridge, 1992.